TISSUE ENGINEERING: Part A
Volume 20, Numbers 11 and 12, 2014
© Mary Ann Liebert, Inc.
DOI: 10.1089/ten.tea.2013.0157

Combined Effect of Three Types of Biophysical Stimuli for Bone Regeneration

Kyung Shin Kang, PhD,[1] Jung Min Hong, PhD,[1] Young Hun Jeong, PhD,[2] Young-Joon Seol, PhD,[3] Woon-Jae Yong, MS,[1] Jong-Won Rhie, MD, PhD,[4] and Dong-Woo Cho, PhD[1]

Pretreatment using various types of biophysical stimuli could provide appropriate potential to cells during construction of the engineered tissue *in vitro*. We hypothesized that multiple combinations of these biophysical stimuli could enhance osteogenic differentiation *in vitro* and bone formation *in vivo*. Cyclic strain, an electromagnetic field, and ultrasound were selected and combined as effective stimuli for osteogenic differentiation using a developed bioreactor. Here we report the experimental evaluation of the osteogenic effects of various combinations of three different biophysical stimuli *in vitro* and *in vivo* using human adipose-derived stem cells (ASCs). Osteogenic differentiation of ASCs was accelerated by multiple-combination biophysical stimulation *in vitro*. However, both single stimulation and double-combination stimulation were sufficient to accelerate bone regeneration *in vivo*, while the osteogenic marker expression of those groups was not as high as that of triple-combination stimulation *in vitro*. We inferred from these data that ASCs appropriately differentiated into the osteogenic lineage by biophysical stimulation could be a better option for accelerating bone formation *in vivo* than relatively undifferentiated or completely differentiated ASCs. Although many questions remain about the mechanisms of combined effects of various biophysical stimuli, this approach could be a more powerful tool for bone tissue regeneration.

Introduction

An appropriate combination of cells, scaffolds, and signals is critical for successful tissue regeneration.[1,2] Among these three components, scaffolds and signals are essential to build new tissues both *in vitro* and *in vivo*. Although there are some studies reporting new tissue regeneration without cells *in vivo*, cells are indispensable to constructing the engineered tissue *in vitro*. Exogenous cells can be implanted with an expectation of specific functions, while host cells have been known to play a principal role in tissue reconstruction. Researchers have generally used exogenous cells matured for their target tissues, for example, osteoblasts for bone regeneration and endothelial cells for vascularization. However, it has been controversial whether undifferentiated stem cells or matured (or differentiated) cells are better suited for target tissue regeneration.[1–6]

To induce cellular maturation (or differentiation) of target tissue, many types of signals have been actively studied according to the target tissues. A growth factor such as bone morphogenetic protein (BMP)-2 is an exemplary signal for inducing osteogenic differentiation for bone tissue.[7–9] This growth factor is a powerful and widely used method for modification of cell types, although there is concern over inflammatory responses.[10,11] On the other hand, biophysical signals have also been studied as effective tools for this purpose. These biophysical signals can stimulate and assist osteogenic differentiation *in vitro* and bone formation *in vivo*.

Strains (such as compressive, tensile, and shear strains), an electromagnetic field, and ultrasound are well-known biophysical stimuli used for bone tissue regeneration. Cyclic strain is one of the biomimetic stimuli that is experienced by bone cells during the daily activities of an organism and is used for bone healing. On the other hand, an electromagnetic field and ultrasound are nonbiomimetic stimuli frequently used for treatment of bone fracture. Even though these stimuli are effective for enhancing osteogenic differentiation and bone formation,[12–16] there are still only a few articles reporting the effects of combining two or more stimuli.[17–19]

In this study, we hypothesized that combinations of these biophysical stimuli would be more powerful for osteogenic differentiation and bone formation than single stimuli. Cyclic strain, an electromagnetic field, and ultrasound were

[1]Department of Mechanical Engineering, Pohang University of Science and Technology (POSTECH), Pohang, Republic of Korea.
[2]Department of Mechanical Engineering, Korea Polytechnic University, Siheung, Republic of Korea.
[3]Wake Forest Institute for Regenerative Medicine, Wake Forest School of Medicine, Medical Center Boulevard, Winston-Salem, North Carolina.
[4]Department of Plastic Surgery, College of Medicine, The Catholic University of Korea, Seoul, Republic of Korea.

selected and combined because of their positive role into inducing the osteogenic potential. To expose the cells to these biophysical stimuli in combinations, a bioreactor was constructed and characterized. In this study, we report the experimental evaluation of the effects of various combinations of three different biophysical stimuli on osteogenic differentiation *in vitro* and bone formation *in vivo* using human adipose-derived stem cells (hASCs).

Materials and Methods

Ethics statement

This study was approved by the Institutional Review Board of Seoul St. Mary's Hospital/Pohang University of Science and Technology (POSTECH) and conformed to the principles expressed in the Declaration of Helsinki. The patient provided written informed consent for cell collection and subsequent analyses.

Isolation and culture of ASCs

hASCs were isolated from one donor and were cultured as described previously.[20,21] The isolated ASCs were cultured in Dulbecco's modified Eagle's medium (Gibco BRL, Grand Island, NY) containing 10% (v/v) fetal bovine serum (Gibco BRL), 100 U/mL penicillin, and 100 μg/mL streptomycin (Gibco BRL) at 37°C in a humidified atmosphere containing 5% CO_2. All experiments were performed at passage 3. Osteogenic differentiation was induced by the osteogenic induction medium containing 10 nM dexamethasone (Sigma-Aldrich, St. Louis, MO), 10 mM β-glycerol phosphate (Sigma-Aldrich), and 50 μg/mL ascorbic acid-2-phosphate (Sigma-Aldrich). All experiments were performed at passage 3.

Development of the bioreactor for triple-combination of stimuli

We previously developed a cyclic strain generator using a flexure-based translational nanoactuator for realizing smooth displacement at the subnanometer to micrometer scale.[22] To combine the generated cyclic strain with ultrasound and electromagnetic field, we modified the previous cyclic strain generator (Fig. 1a). The piezoactuators were inserted in the push rods to generate and transfer an ultrasonic signal to the cells (Fig. 1b). The whole device was developed using nonconductive materials so that we could minimize the distortion of the electromagnetic signals. This cyclic strain and ultrasound generating platform was located inside the custom-made solenoid coil for the electromagnetic exposure to cells (Fig. 1c). The inner diameter and length of the solenoid coil were 180 and 400 mm, respectively. Three-axis magnetic field sensor (MFS-3A; Ametes, San Carlos, CA) was used to measure the magnetic flux density. We identified cyclic strain signal changes under the electromagnetic field or/and ultrasound using a capacitive displacement sensor (4810 with 2805; MicroSense, LCC, Lowell, MA). The acoustic output power of the transducer was measured using an acoustic force balance (UPM-DT-1AV; Ohmic Instruments Co., Easton, MD). Intensity was expressed by the spatial average temporal average. The whole bioreactor system was in a humidified incubator at 37°C containing 5% CO_2.

Fabrication of 3D PCL/PLGA/TCP scaffolds

A customized multihead deposition system was used to fabricate 3D scaffolds as described previously.[20] For the mouse calvarial defect model, we designed the scaffold to fit the critical defect size (diameter: 4 mm). The thickness was 1 mm with 10 layers of 100 μm. The line width and pore size were 300 and 300 μm, respectively (Fig. 1d). The scaffold materials were prepared with a blend of polycaprolactone (PCL, Mw 45,000–60,000; Sigma-Aldrich), 85:15 poly(lactic-co-glycolic acid) (PLGA, Mw 50,000–75,000; Sigma-Aldrich), and tricalcium phosphate (TCP; Berkeley Advanced Biomaterials, Inc., Berkeley, CA) with a ratio of 40:40:20 (PCL:PLGA:TCP) to enhance the biological and mechanical properties of the scaffolds.[23] Three-dimensional PCL/PLGA/TCP scaffolds were fabricated by dispensing the molten polymer at 120°C through the nozzle with the pneumatic pressure (650 kPa) and stacking each layer. We used a code generation algorithm modified from the previously developed one.[24] The scaffold morphology was examined using a scanning electron microscope (JSM-5300; Jeol, Tokyo, Japan) operated at 15 kV.

Stimulation of cells by each stimulus

ASCs were seeded at a density of 2×10^4 cells/scaffold onto the 3D PCL/PLGA/TCP scaffolds. After submerging the scaffolds in 70% alcohol for 2 h, they were sterilized using UV light (intensity: 40 W, dose: 26,272 mJ/cm^2) for 1 h. Then, they were washed three times using phosphate-buffered saline (PBS) without drying. The ASC-seeded 3D PCL/PLGA/TCP scaffolds were located on the 12-well plate, which was in the center part of the cyclic strain generator. The height of each push rod was adjusted just to the top surface of each scaffold with initial static clamping. The ASCs on the scaffolds were exposed to the cyclic strain for 1 h per day during the experimental periods. The frequency and the magnitude of the cyclic strain were 1 Hz and 0.3%, respectively. For the ultrasound, the cells were treated for 20 min per day at a 1.5-MHz frequency and 30-mW/cm^2 intensity.[21] A 45-Hz electromagnetic field was applied at 1 mT for 8 h per day.[25] We did not consider time-dependent orders of the treatment using each stimulus. Every stimulus was applied to cells simultaneously for multiple-combination stimulation. Seven different combinations were compared with one another, as shown in Table 1. All experiments were conducted under conditions without heat generation.

Real-time polymerase chain reaction

Total RNA (1 μg) was extracted from cultured cells using the TRIzol reagent (Invitrogen, Groningen, Netherlands) and was used as a template for cDNA synthesis (Invitrogen, Eugene, OR). Real-time polymerase chain reaction (PCR) was performed using a SYBR Green PCR Master Mix assay (Applied Biosystems, Warrington, United Kingdom) and ABI StepOnePlus system (Applied Biosystems, Foster City, CA). After the initial step at 95°C for 10 min, the amplification reaction was performed for 40 cycles with denaturation at 95°C for 15 s and annealing at 60°C for 1 min. The following primers were used: GAPDH sense, 5′-CCAGGTGGTCTCCTCTGACTTC-3′; GAPDH antisense,

Table 1. Description of Experimental Groups for *In Vitro* Evaluation

Group	*Combination type*	*Description*
Control	—	No stimulation
C	Single	Cyclic strain
E	Single	Electromagnetic field
U	Single	Ultrasound
CE	Double	Cyclic strain + electromagnetic field
CU	Double	Cyclic strain + ultrasound
EU	Double	Electromagnetic field + ultrasound
CEU	Triple	Cyclic strain + electromagnetic field + ultrasound

5′-GTGGTCGTTGAGGGCAATG-3′; alkaline phosphatase (ALP) sense, 5′-ATGTCATCATGTTCCTGGGAGAT-3′; ALP antisense, 5′-TGGAGCTGACCCTTGAGGAT-3′; heat-shock protein 27 (HSP27) sense, 5′-CCCTGGATGTCAAC-CACTTC-3′; HSP27 antisense, 5′-TCTCCACCA CGCCA TCCT-3′; osterix (OSX) sense, 5′-GGCAGCG TGCAGC AAATT-3′; and OSX antisense, 5′-CCTGCTT TGCCCAG AGTTGT-3′.

RUNX2 staining

After fixation with 4% paraformaldehyde solution for 30 min, the samples were embedded in the O.C.T. compound embedding medium (Tissue-Tek; Sakura Fineteck, Inc., Torrance, CA). Then, 5-μm sections were prepared using a cryostat (Leica, Wetzlar, Germany). The slides were permeabilized with 0.1% Triton X-100 and blocked with 0.2% bovine serum albumin for 15 min. They were then incubated with anti-RUNX2 (Santa Cruz, Heidelberg, Germany) (primary antibody). After washing with PBS, a secondary antibody (Alexa 488 anti-rabbit, diluted 1:200) was added and the samples were incubated for 1 h at room temperature. The samples were mounted with the antifade reagent (Invitrogen, Eugene, OR) and observed using a FluoView 1000 confocal microscope (Olympus, Melville, NY). All images were captured without changing the camera settings.

Cell viability assay

Cell viability was measured using the 3-(4,5-dimethylthiazol-2-yl)-5-(3-carboxymethoxyphenyl)-2-(4-sulfophenyl)-2H-tetrazolium (MTS) assay, which is a colorimetric method used for measuring the number of viable cells in proliferative or cytotoxic conditions. After culturing for 7 days, the cells were incubated in 25 μM/well of MTS solution (5 mg/mL) for 2 h at 37°C. The culture medium was then replaced with 100 μL of extraction buffer (20% sodium dodecyl sulfate and 50% N,N-dimethylformamide) to dissolve formazan crystals, and the absorbance was measured at 490 nm using a microplate reader.

For DNA quantification, total DNA was extracted from the scaffolds using Tris EDTA and Proteinase K after 7 days. After mixing with distilled water, the DNA content was measured using a Nanodrop ND1000 spectrophotometer (NanoDrop Technologies, Wilmington, DE).

In vivo *implantation*

These animal study procedures were approved by the Institutional Animal Care and Use Committee at POSTECH. Immunodeficient BALB/cAnN.Cg mice (6-week-old males; Orient Bio, Seoungnam, Korea) were anesthetized with an intraperitoneal injection of avertin (240 mg/kg; Sigma-Aldrich). Full-thickness critical-sized calvarial defects (4 mm diameter) were created in the central parietal bone using a trephine bur. The ASCs on the PCL/PLGA/TCP scaffolds were stimulated for 7 days using various combinations of the three types of stimuli *in vitro* as shown in Table 2. Subsequently, we implanted these pretreated ASC-seeded PCL/PLGA/TCP scaffolds in the calvarial defects ($n = 5$ per group). Finally, the skin was closed with 4-0 nylon sutures. The mice were sacrificed and the implants were retrieved 8 weeks after surgical implantation.

Microcomputed tomography, histology, and immunohistochemistry analyses

All samples were fixed with 10% formalin for 12 h at 4°C and washed several times with PBS. They were scanned using microcomputed tomography (CT) (Skyscan 1076; Skyscan, Aartselaar, Belgium) with an X-ray source of 60 kV and167 μA. After scanning, 3D images were reconstructed using cross-sectional slices and their threshold values were from 0 to 0.18.

These fixed samples were dehydrated through an ethanol gradient and embedded in Technovit 9100 New (Heraeus Kulzer GmbH, Hanau, Germany) for the histological analysis. The embedded samples were sectioned with a microtome and cut at 5 μm, then stained with hematoxylin and eosin. The stained sample images were obtained using a microscope (ELIPSE Ti-S; Nikon Instruments, Inc., Melville, NY).

The sections were stained with anti-lamin A/C (Abcam, Cambridge, MA) as a marker for human-specific cell detection, followed by anti-mouse IgG conjugated with TRITC (Molecular Probes, Eugene, OR). Additionally, the sections were stained with anti-CD31 (Abcam) followed by FITC (Molecular Probes) to observe vascularization after the implantation of exogenous cells on the scaffolds. The anti-lamin A/C-stained sections were stained with DAPI and mounted with the antifade reagent (Invitrogen, Carlsbad, CA). DAPI, which binds to the AT-rich regions of DNA,[26] was used to observe the nuclei of the cells. The images were observed using a FluoView 1000 confocal microscope (Olympus). All the images were captured without changing the camera settings.

Table 2. Description of Pretreatment Groups for *In Vivo* Evaluation

Group	*Scaffold*	*Cell*	*Pretreatment*
Blank	×	×	×
Control	○	○	×
C	○	○	Cyclic strain (C)
E	○	○	Electromagnetic field (E)
CE	○	○	C + E
CEU	○	○	CE + ultrasound

×, not included; ○, included.

Results

Characterization of bioreactor

The bioreactor was developed for stimulating cells with the three different biophysical stimuli simultaneously (Fig. 1). The platform that generates the cyclic strain and ultrasound was positioned in the area where the uniform electromagnetic field was guaranteed to be within a ±5% error.[27] We identified the generated signals to validate each biophysical stimulus and checked any unexpected interference caused when two or three stimuli were applied simultaneously.

Figure 2 shows that the stimulation signals could be applied to the ASCs on the 3D scaffolds and that those signals were independent of one another. The magnetic flux density was not affected by generating the cyclic strain or ultrasound (Fig. 2a, b). In addition, we observed that the controllable cyclic strain (displacement) was generated securely regardless of the electromagnetic field without ultrasound (Fig. 2c). When ultrasound was applied, additional displacement with a higher frequency and smaller magnitude was generated (Fig. 2d). This displacement was superimposed on the cyclic strain signals. However, the ultrasound-induced displacement was negligible in the power spectral expression. Additionally, the frequency and magnitude of the cyclic strain displacement were not affected by this ultrasound-induced vibration. Figure 2e shows the performance of the ultrasonic push rods, which was expressed using ultrasonic intensity according to the input voltage.

Osteogenic differentiation promoted by multiple-combination biophysical stimulation

We measured osteogenic mRNA expression using real-time PCR to observe the effect of various combinations of the three types of biophysical stimuli as shown in Figure 3. ASCs seeded on the 3D PCL/PLGA/TCP scaffolds were exposed to the biophysical stimuli with defined stimulation conditions (Table 1). All combinations of biophysical stimuli could increase ALP and OSX expression levels regardless of stimulation types. Both double and triple combinations showed higher ALP and OSX expression than those of the single stimulation groups. The ALP expression level in the cyclic strain + electromagnetic field + ultrasound (CEU) group was significantly higher than the ALP expression levels in the double-combination groups, whereas the enhancement of the OSX expression level in the CEU was not significant compared with the OSX expression levels in the double-combination groups. The differences in gene expression of group C compared with groups E or U

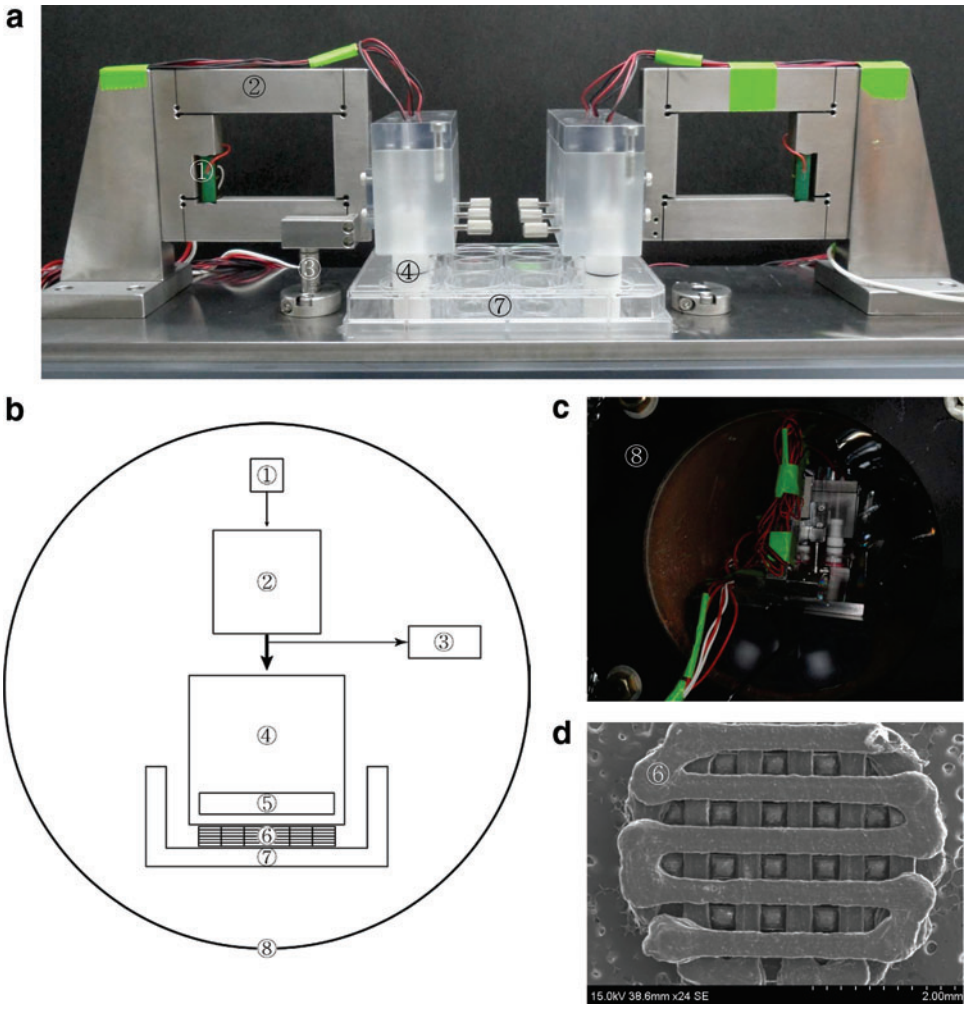

FIG. 1. Bioreactor for generating multiple-combination biophysical stimulation and 3D PCL/PLGA/TCP scaffold. **(a)** Previously developed flexure-based cyclic stain bioreactor was modified. **(b)** Schematic diagram shows how cells on the scaffold were stimulated using the developed bioreactor. **(c)** The whole device was exposed to the electromagnetic field inside the solenoid coil. **(d)** Scanning electron microscope images of 3D PCL/PLGA/TCP scaffolds with original magnification, 24×. ①: piezoelectric actuator, ②: translational nanoactuator, ③: capacitive displacement sensor, ④: push rod, ⑤: ultrasonic transducer, ⑥: scaffold, ⑦: 12-well plate, ⑧: solenoid coil. PCL, polycaprolactone; PLGA, poly(lactic-co-glycolic acid); TCP, tricalcium phosphate. Color images available online at www.liebertpub.com/tea

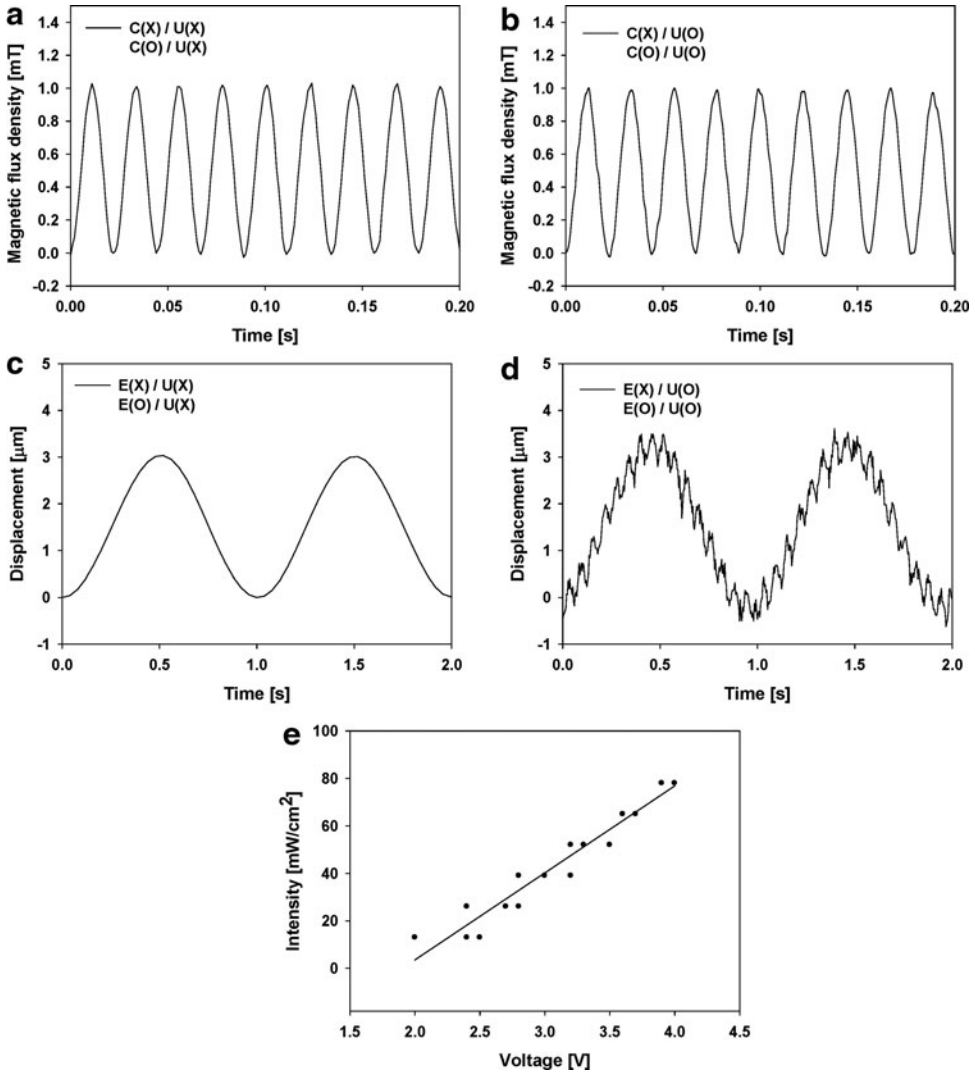

FIG. 2. Identification of each biophysical stimulus. **(a, b)** Magnetic flux density was measured with combinations of cyclic strain and ultrasound using magnetic sensors. **(c, d)** Cyclic strain (displacement) was measured with combinations of electromagnetic field and ultrasound using capacitive displacement sensors. **(e)** Ultrasonic intensity (acoustic pressure) generated from the push rod module was measured using an acoustic force balance. C, cyclic strain; E, electromagnetic field; U, ultrasound; X, was not generated; O, was generated.

among the single stimulation groups were not significant, whereas gene expression in E was significantly higher than that of U. Likewise, the differences of expression levels of both ALP and OSX among the double-combination groups were not statistically significant.

The pattern of RUNX2 expression was similar to the pattern of ALP and OSX expression (Fig. 3). Figure 4 shows that all the combinations of biophysical stimuli enhanced RUNX2 expression compared with the control group (unstimulated group). Only the expression level of U was slightly lower compared with other single-combination groups (C and E). Although multiple-combination groups showed higher RUNX2 expression compared with single stimulation groups, it was difficult to find strong induction of RUNX2 expression in the triple-combination groups compared with the double-combination groups.

After biophysical stimulation, we evaluated HSP27 expression to assess the stress response of cells caused by multiple combinations of stimuli. The single stimulation groups did not show any differences in HSP27 compared with the control group, as shown in Figure 5a. The HSP27 level was lower in the two double-combination groups (CE and EU), but the difference was not significant. HSP27 expression was remarkably lower than the other groups when ASCs were exposed to CEU stimulation. In the CEU group, this result correlates with the reduced cell viability and DNA content of the ASCs after stimulation for 7 days (Fig. 5b, c).

Bone formation affected by multiple types of biophysical stimuli

We verified enhancement of regeneration of mouse calvarial bone by *in vitro* pretreatment of ASCs using various combinations of three types of stimuli. ASCs seeded on 3D PCL/PLGA/TCP scaffolds were stimulated using the selected biophysical stimuli for 1 week before implantation (Table 2). For the simplified experiment using the single- and double-combination groups, a stimulus group (U) was omitted because other combination groups showed similar gene expression patterns *in vitro*. For example, RUNX2 expression was similar between the C, E, and U groups and between the CE, CU, and EU groups. Therefore, C was selected because it was the only biomimetic stimulus, and U was omitted because both C and U were vibration-based stimuli. Micro-CT images in Figure 6 show that the E and

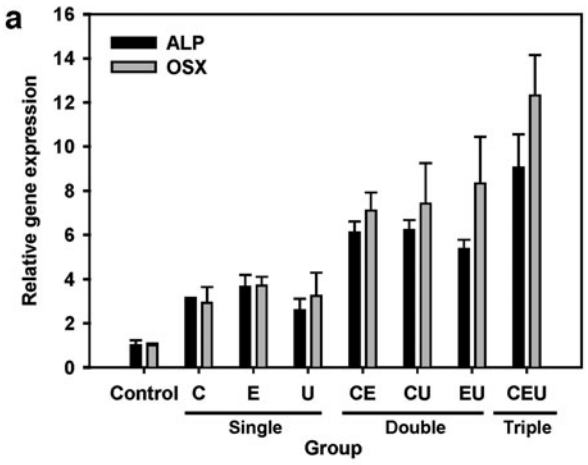

b **Significance on ALP**

P value	Control	C	E	U	CE	CU	EU	CEU
Control		0.000	0.001	0.005	0.000	0.000	0.000	0.001
C			**0.074**	**0.130**	0.000	0.000	0.000	0.000
E				0.046	0.004	0.003	0.012	0.004
U					0.000	0.000	0.001	0.000
CE						**0.780**	**0.117**	0.032
CU							**0.069**	0.035
EU								0.015

Significance on OSX

P value	Control	C	E	U	CE	CU	EU	CEU
Control		0.010	0.000	0.016	0.000	0.007	0.004	0.001
C			**0.092**	**0.678**	0.003	0.027	0.014	0.003
E				**0.388**	0.000	0.004	0.002	0.000
U					0.003	0.020	0.008	0.001
CE						**0.801**	**0.404**	0.020
CU							**0.658**	**0.116**
EU								**0.120**

FIG. 3. Gene expression affected by various combinations of three biophysical stimuli. **(a)** ALP and OSX expression was measured at day 7 using real-time PCR. **(b)** *p*-Values were calculated to compare all the experimental groups individually. Bold characters indicate *p*-values higher than 0.05. PCR, polymerase chain reaction; ALP, alkaline phosphatase; OSX, osterix.

CE groups had a larger volume of bone tissue than other stimulation groups, even though all of the stimulation groups promoted bone formation.

The histological evaluation revealed that pretreatment using biophysical stimulation enhanced new bone formation as described in Figure 7. A large amount of new bone was formed in the space among the scaffold struts when the ASCs were stimulated. However, newly formed bone was not dense in the control group. E and CE showed more matured bone tissue compared with the other stimulation groups. Although CEU showed a stronger capacity for bone regeneration compared with the unstimulated group, its effect seemed to be weaker than E or CE alone.

The human-specific lamin A/C antibody stains human cells among heterogeneous tissue,[27] which demonstrated that a portion of the implanted hASCs remained for 8 weeks. The nuclei of both mouse and human cells are responsive to DAPI staining.[26,28,29] In this study, the number of mouse and human cells seemed to be similar through all experimental groups except group C (Fig. 8). The number of nuclei in the group C was higher than that in the other groups. Among the blank and control group cells that were stained with DAPI, the lamin A/C staining revealed that the implanted ASCs did not exist, whereas the pretreated ASCs were detected. Compared with the CEU group, a higher lamin A/C expression was observed in the C (2.3), E (3.67), and CE (1.58) groups, which also showed a higher degree of bone formation than the CEU group (Figs. 7 and 8). Unexpectedly, we were not able to observe a large distribution of lamin A/C in the CEU group (0.56), although the osteogenic marker expression in this group was the highest (Fig. 3).

CD31 expression, a respresentative vascularization marker,[30] was used to characterize vascularization 8 weeks after the implantation of exogenous ASCs. The expression of CD31 was higher in the single- (C and E) and double-combination (CE) groups compared with the unstimulated group (control) (Fig. 8). However, the CD31 expression in the CEU group (4.71) was not to be stronger than CD31 expression in the CE group (7.88).

Discussion

Biophysical stimulation is an effective method for enhancing osteogenic differentiation *in vitro* and bone formation *in vivo*. Among various types of biophysical stimuli, the three individual types of stimuli selected for this study have been proven to have positive effects on osteogenic potential.[12–16] We hypothesized that combining these biophysical stimuli could be a more powerful method for enhancing osteogenic potential induced by each individual stimulus synergistically.[17] The developed bioreactor was able to generate and transfer both individual and combined biophysical signals using three different stimuli to cells on the 3D scaffolds. This study used previously selected stimulation conditions.

Osteogenic differentiation was accelerated by multiple-combination biophysical stimulation *in vitro*. First, we confirmed that even a single stimulus had a positive effect on osteogenic marker expression compared with the unstimulated group in our experimental setup. When these stimuli were combined, they yielded a synergistic effect. The double- and triple-combination biophysical stimulation groups showed a higher ALP and OSX expression than any single-stimulation group. However, stimulation with any of the three types of stimuli alone or combined in pairs did not make remarkable differences in osteogenic marker expression.

Osteogenic marker expression *in vitro* suggested that osteogenic differentiation status might differ at the same point in time according to the types of biophysical combinations. Both double- and triple-combination stimulation accelerated osteogenic differentiation compared with the unstimulated (control) or the single-stimulation groups because a higher expression of ALP and RUNX2 is reflective of more rapid osteogenic differentiation of ASCs.[31,32] Surprisingly, our *in vivo* data indicated that the higher expression of osteogenic markers *in vitro* did not guarantee a higher degree of bone formation *in vivo*. Although the

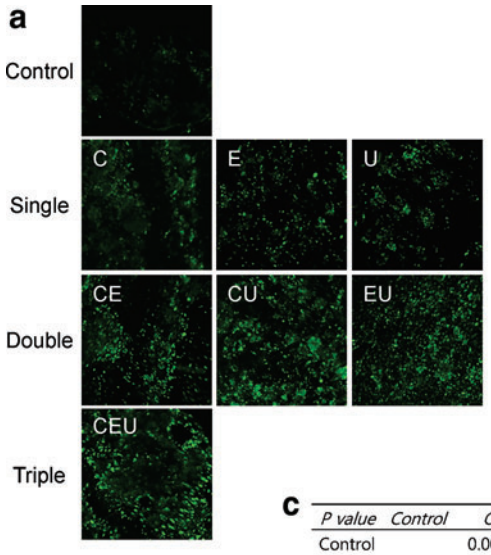

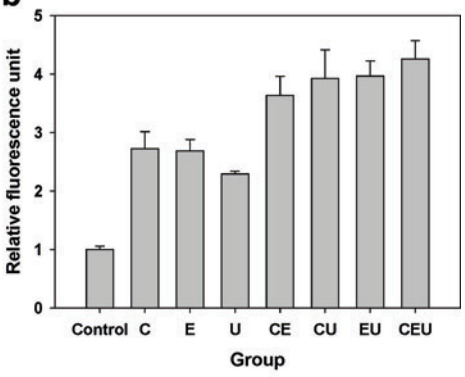

c

P value	*Control*	*C*	*E*	*U*	*CE*	*CU*	*EU*	*CEU*
Control		0.000	0.000	0.000	0.000	0.000	0.000	0.000
C			**0.840**	0.026	0.011	0.004	0.002	0.001
E				0.007	0.005	0.002	0.001	0.000
U					0.000	0.000	0.000	0.000
CE						**0.407**	**0.242**	**0.077**
CU							**0.900**	**0.342**
EU								**0.285**

FIG. 4. Induced RUNX2 expression by various combinations of three types of biophysical stimuli. **(a)** RUNX2 expression was analyzed using immunostaining at day 7. Original magnification, 800×. **(b)** RUNX2 expression was quantified. **(c)** *p*-Values were calculated to compare all the experimental groups individually. Bold characters indicate *p*-values higher than 0.05. Color images available online at www.liebertpub.com/tea

osteogenic marker expression level in the CEU group was the highest *in vitro*, the E (single) and CE (double) groups showed a higher degree of new bone formation than the CEU group (triple) *in vivo*.

Selecting undifferentiated stem cells or osteoblasts as the cell source for bone tissue regeneration remains controversial.[3] Meinel *et al.* and Peister *et al.* reported that predifferentiated mesenchymal stem cells (MSCs) could enhance bone formation,[33,34] whereas Castano-Izquierdo *et al.* showed that undifferentiated MSCs were more effective than osteoblasts.[35] The possible role of exogenous cells in bone formation has been described as a mediator of recruitment of circulating cells and direct bone formation.[4,6,36] Tortelli *et al.* reported that implanted MSCs and osteoblasts induced new bone formation of different origins, specifically endochondral and intramembranous ossification, respectively.[4]

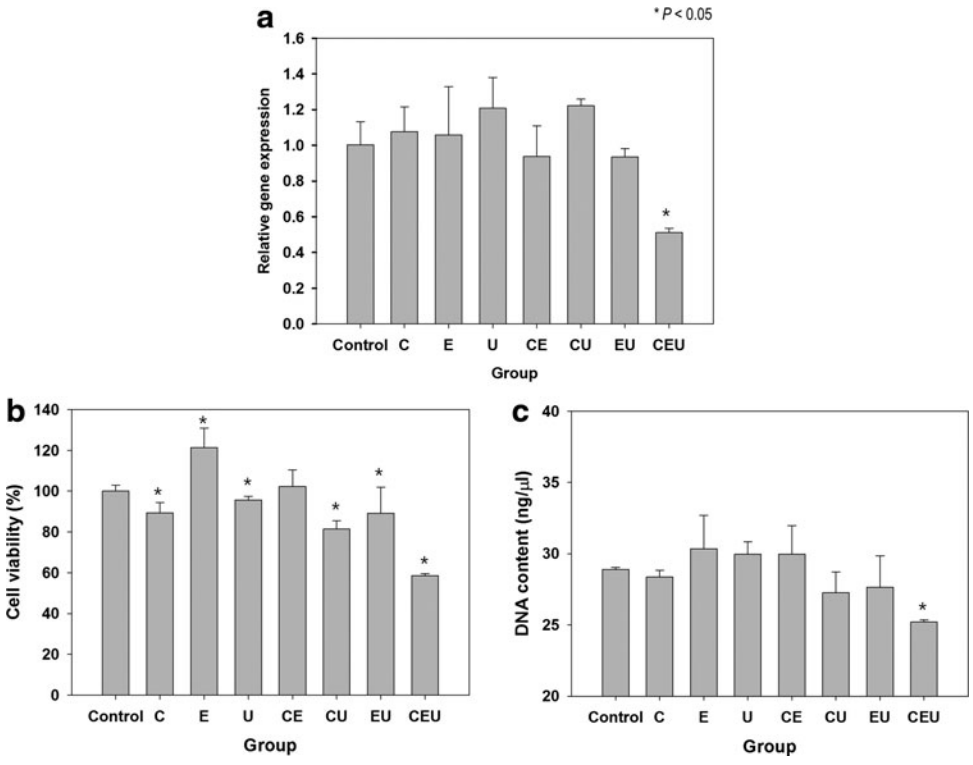

FIG. 5. Effect of triple-combination stimulation on cellular stress and viability. **(a)** Stress-related gene expression (HSP27) was measured by real-time PCR at day 7. A significant decrease in HSP27 was observed in the CEU group, which indicates that the triple-combination stimulation might induce cellular stress. **(b)** Cell viability in the CEU group was lower at day 7 than that in the control and other experimental groups. **(c)** DNA content was measured at day 7. The detected DNA amount decreased significantly in the CEU group compared with the control. $^*p < 0.05$. HSP27, heat-shock protein 27; CEU, cyclic strain + electromagnetic field + ultrasound.

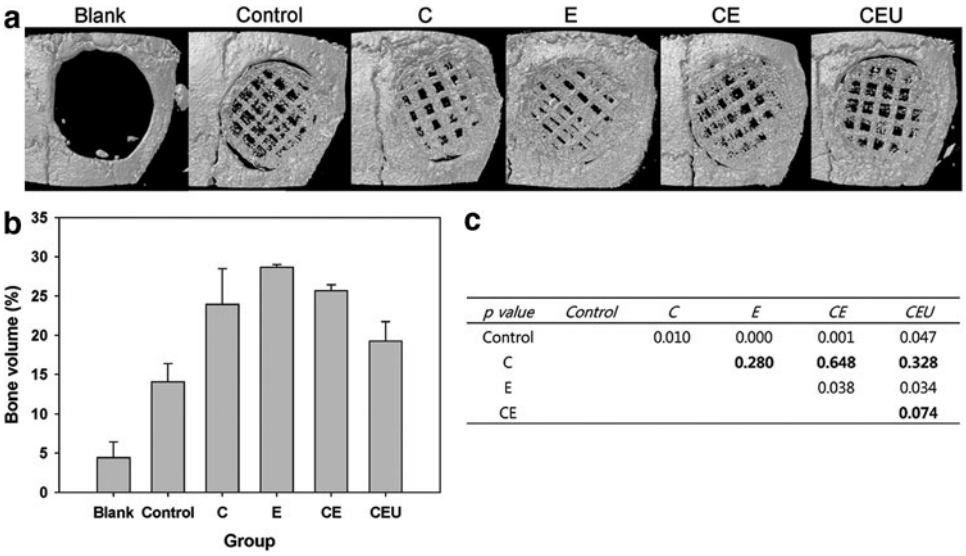

c

p value	*Control*	*C*	*E*	*CE*	*CEU*
Control		0.010	0.000	0.001	0.047
C			**0.280**	**0.648**	**0.328**
E				0.038	0.034
CE					**0.074**

FIG. 6. Radiographic analysis of bone formation. **(a)** Microcomputed tomography images were taken after 8 weeks. **(b)** The bone volume of each group was calculated. **(c)** *p*-Values were calculated to compare all the experimental groups individually. Bold characters indicate *p*-values higher than 0.05.

Our data showed a possibility that the regeneration of host tissue might be dependent on how much ASCs were induced to differentiate into the osteogenic lineage. The appropriate motivation (E or CE) of ASCs to differentiate into the osteogenic lineage seemed to promote a higher bone formation than less differentiated (control) or completely differentiated ASCs (CEU). These ASCs appropriately induced differentiation into osteogenic lineage (i.e., ASCs midway through osteogenic differentiation), which seemed to induce greater vascularization than those of the other experimental groups. Undifferentiated MSCs have been described as contributing to bone formation by secreting paracrine factors, leading to ingrowth of blood vessels or associated perivascular stem cells.[36] However, our CD31 expression showed that vascularization was weak in the control, which was similar to undifferentiated ASCs.

Additionally, the survival of the donor ASCs is possibly related to this level of differentiation. It can be noted from the lamin A/C staining that the relatively larger number of implanted ASCs in the E and CE groups remained, while almost no implanted cells did in the other groups. Although populations of exogenous cells have been proven to decrease during bone formation,[4,37] we observed some implanted cells (E or CE) that survived longer than the less differentiated cells (control).

Expression of a stress-related gene, HSP27, decreased when ASCs were treated with triple-combination biophysical stimulation (CEU), whereas the other combinations of stimuli did not affect HSP27 expression significantly. We believe that the decreased HSP27 expression could increase the possibility of apoptosis of ASCs after exposure to the triple-combination biophysical stimuli because downregulated HSP27 could promote stress-induced intrinsic cell death and reduced cell survival after stress.[38,39] The cell viability results confirmed that the CEU stimulation decreased the ASC survival rate, which indicated that the triple-combination

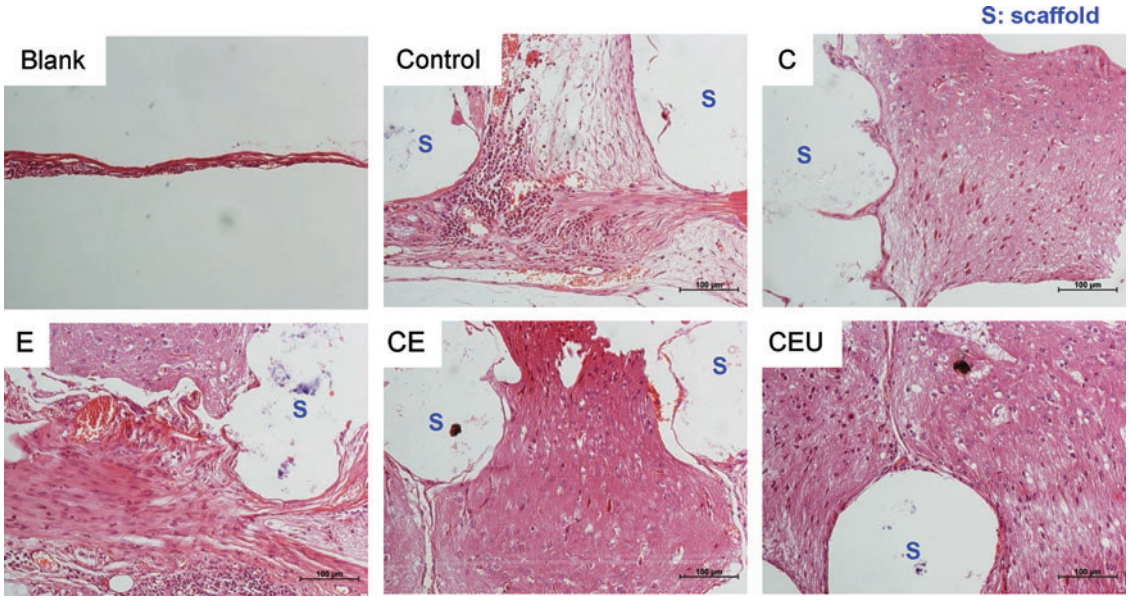

FIG. 7. Histological analysis of bone formation at week 8 (H&E). Newly formed bone tissue near the scaffold struts was observed at a higher density in E and CE. S, scaffold. Color images available online at www.liebertpub.com/tea

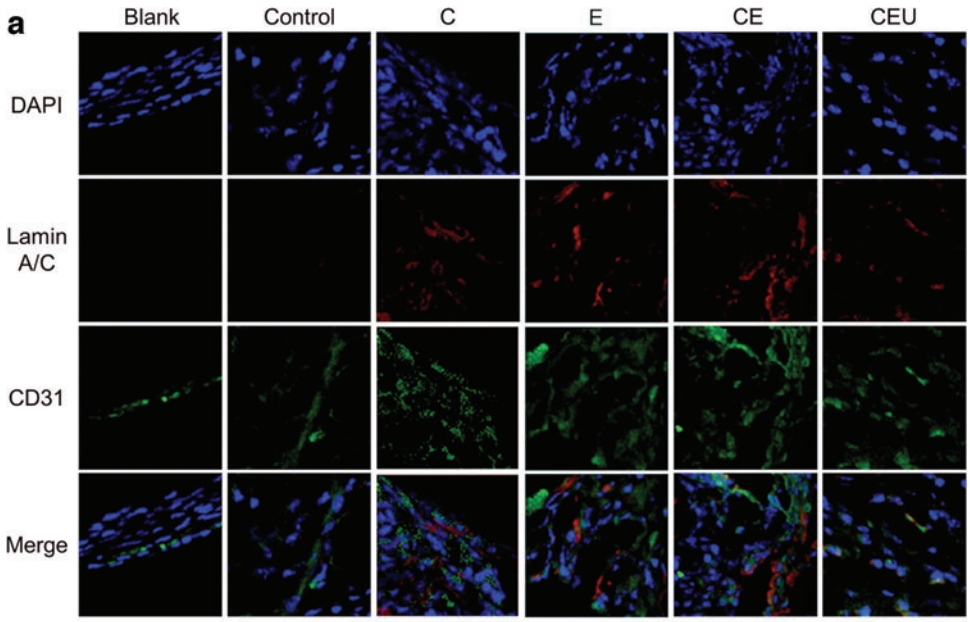

b

Protein \ Group	Blank	Control	C	E	CE	CEU
DAPI	11.92	10.04	14.65	10.18	9.24	12.73
Lamin A/C	-	-	2.30	3.67	1.58	0.56
CD31	2.53	4.60	9.07	9.16	7.88	4.71

FIG. 8. Immunohistochemistry images of human lamin A/C and CD31 at week 8. **(a)** Green and red colors indicated stained CD31- and human-specific lamin A/C, respectively. Nuclei were expressed with DAPI (blue color). Original magnification, 400×. **(b)** DAPI, lamin A/C, and CD31 fluorescence is quantified in the table. Color images available online at www.liebertpub.com/tea

stimulation caused cellular stress *in vitro*. Even though triple-combination biophysical stimulation could increase osteogenic marker expression, it might risk triggering some cell death at the same time. It may be that this risk could somewhat affect *in vivo* new bone formation after pretreatment.

Even though both double and triple stimulation types were combinations of more than two different types of stimuli, only under the triple-combination stimulation did we observe the decreased cell viability. This effect could be influenced by decreased HSP27 expression only under the triple-combination stimulation. We infer that this could be associated with the different energy level depending on the combination type and the energy level criterion triggering HSP27 downregulation, which would have been somewhere between the energy level of double stimulation and that of triple stimulation. Therefore, the higher energy level of triple stimulation than the certain criterion would trigger HSP27 downregulation, whereas the energy level of the double stimulation could not.

Although many questions remain about the mechanisms of the combined effects of various biophysical stimuli, we were able to evaluate the pretreatment effect using combinations of multiple types of biophysical stimuli *in vitro* and *in vivo*. Our data indicated that single- or double-combination stimulation was sufficient to accelerate bone regeneration, while osteogenic marker expression in these groups was not higher compared with the triple-combination stimulation group. We inferred that appropriately differentiated ASCs might be a better option for accelerating bone formation *in vivo* rather than undifferentiated or further differentiated ASCs.

Future studies will be necessary to evaluate multiple-combination biophysical stimulation with various orders of different stimulations, whereas only simultaneous stimulation combinations were investigated in this article. The order, duration, and rest period for determining stimulation combinations would be essential factors to be considered. The triple-combination biophysical stimulation could be a better option for bone formation, provided that the appropriate determination of these factors might reduce the stress effect of multiple-combination stimulation. Moreover, pretreatment using multiple-combination biophysical stimulation with the appropriate dose of growth factors, such as BMP-2, could provide a more powerful stimulation platform for accelerating bone tissue regeneration.

Acknowledgments

This work was supported by the National Research Foundation of Korea (NRF) grant funded by the Korea government (MSIP) (No. 2010-0018294 and 2011-0030075).

Disclosure Statement

No competing financial interests exist.

References

1. Kneser, U., Schaefer, D.J., Polykandriotis, E., and Horch, R.E. Tissue engineering of bone: the reconstructive surgeon's point of view. J Cell Mol Med **10,** 7, 2006.
2. Chen, F.H., Rousche, K.T., and Tuan, R.S. Technology insight: adult stem cells in cartilage regeneration and tissue engineering. Nat Clin Pract Rheum **2,** 373, 2006.

3. Rai, B., Lin, J.L., Lim ZXH, Guldberg, R.E., Hutmacher, D.W., and Cool, S.M. Differences between *in vitro* viability and differentiation and *in vivo* bone-forming efficacy of human mesenchymal stem cells cultured on PCL-TCP scaffolds. Biomaterials **31,** 7960, 2010.
4. Tortelli, F., Tasso, R., Loiacono, F., and Cancedda, R. The development of tissue-engineered bone of different origin through endochondral and intramembranous ossification following the implantation of mesenchymal stem cells and osteoblasts in a murine model. Biomaterials **31,** 242, 2010.
5. Li, X.Y., Yao, J.F., Wu, L., Jing, W., Tang, W., Lin, Y.F., *et al.* Osteogenic induction of adipose-derived stromal cells: not a requirement for bone formation in vivo. Artif Organs **34,** 46, 2010.
6. Tasso, R., Augello, A., Boccardo, S., Salvi, S., Carida, M., Postiglione, F., *et al.* Recruitment of a host's osteoprogenitor cells using exogenous mesenchymal stem cells seeded on porous ceramic. Tissue Eng Pt A **15,** 2203, 2009.
7. Urist, M.R., DeLange, R.J., and Finerman, G.A. Bone cell differentiation and growth factors. Science **220,** 680, 1983.
8. Chaudhary, L.R., Hofmeister, A.M., and Hruska, K.A. Differential growth factor control of bone formation through osteoprogenitor differentiation. Bone **34,** 402, 2004.
9. Shanmugarajan, T.S., and Im, G.I. Osteogenic differentiation of mesenchymal stem cells and bone tissue engineering. Tissue Eng Regen Med **8,** 347, 2011.
10. Ritting, A.W., Weber, E.W., and Lee, M.C. Exaggerated inflammatory response and bony resorption from BMP-2 use in a pediatric forearm nonunion. J Hand Surg Am **37A,** 316, 2012.
11. Mountziaris, P.M., and Mikos, A.G. Modulation of the inflammatory response for enhanced bone tissue regeneration. Tissue Eng Part B Rev **14,** 179, 2008.
12. Sant'Anna, E.F., Leven, R.M., Virdi, A.S., and Sumner, D.R. Effect of low intensity pulsed ultrasound and BMP-2 on rat bone marrow stromal cell gene expression. J Orthop Res **23,** 646, 2005.
13. Suzuki, A., Takayama, T., Suzuki, N., Sato, M., Fukuda, T., and Ito, K. Daily low-intensity pulsed ultrasound-mediated osteogenic differentiation in rat osteoblasts. Acta Bioch Bioph Sin **41,** 108, 2009.
14. Rego, E.B., Inubushi, T., Kawazoe, A., Tanimoto, K., Miyauchi, M., Tanaka, E., *et al.* Ultrasound stimulation induces PGE(2) synthesis promoting cementoblastic differentiation through Ep2/Ep4 receptor pathway. Ultrasound Med Biol **36,** 907, 2010.
15. Qi, M.C., Hu, J., Zou, S.J., Chen, H.Q., Zhou, H.X., and Han, L.C. Mechanical strain induces osteogenic differentiation: Cbfa1 and Ets-1 expression in stretched rat mesenchymal stem cells. Int J Oral Maxillofac Surg **37,** 453, 2008.
16. Jagodzinski, M., Breitbart, A., Wehmeier, M., Hesse, E., Haasper, C., Krettek, C., *et al.* Influence of perfusion and cyclic compression on proliferation and differentiation of bone marrow stromal cells in 3-dimensional culture. J Biomech **41,** 1885, 2008.
17. Kang, K.S., Lee, S.J., Lee, H., Moon, W., and Cho, D.W. Effects of combined mechanical stimulation on the proliferation and differentiation of pre-osteoblasts. Exp Mol Med **43,** 367, 2011.
18. Walker, N.A., Denegar, C.R., and Preische, J. Low-intensity pulsed ultrasound and pulsed electromagnetic field in the treatment of tibial fractures: a systematic review. J Athl Training **42,** 530, 2007.
19. Li, J.K.J., Lin, J.C.A., Liu, H.C., Sun, J.S., Ruaan, R.C., Shih, C., *et al.* Comparison of ultrasound and electromagnetic field effects on osteoblast growth. Ultrasound Med Biol **32,** 769, 2006.
20. Hong, J.M., Kim, B.J., Shim, J.H., Kang, K.S., Kim, K.J., Rhie, J.W., *et al.* Enhancement of bone regeneration through facile surface functionalization of solid freeform fabrication-based three-dimensional scaffolds using mussel adhesive proteins. Acta Biomater **8,** 2578, 2012.
21. Kang, K.S., Hong, J.M., Kang, J.A., Rhie, J.W., and Cho, D.W. Osteogenic differentiation of human adipose-derived stem cells can be accelerated by controlling the frequency of continuous ultrasound. J Ultrasound Med **32,** 1461, 2013.
22. Kang, K.S., Jeong, Y.H., Hong, J.M., Yong, W.J., Rhie, J.W., and Cho, D.W. Flexure-based device for cyclic strain-mediated osteogenic differentiation. J Biomech Eng **135,** 114501, 2013.
23. Liu, F.H., Shen, Y.K., and Lee, J.L. Selective laser sintering of a hydroxyapatite-silica scaffold on cultured MG63 osteoblasts in vitro. Int J Precis Eng Man **13,** 439, 2012.
24. Jung, J.W., Kang, H.W., Kang, T.Y., Park, J.H., Park, J., and Cho, D.W. Projection image-generation algorithm for fabrication of a complex structure using projection-based microstereolithography. Int J Precis Eng Man **13,** 445, 2012.
25. Kang, K.S., Hong, J.M., Kang, J.A., Rhie, J.W., Jeong, Y.H., and Cho, D.W. Regulation of osteogenic differentiation of human adipose-derived stem cells by controlling electromagnetic field conditions. Exp Mol Med **45,** e7, 2013.
26. Kapuscinski, J. Dapi—a DNA-specific fluorescent-probe. Biotech Histochem **70,** 220, 1995.
27. Kang, K.S., Hong, J.M., Seol, Y.-J., Rhie, J.-W., Jeong, Y.H., and Cho, D.-W. Short-term evaluation of electromagnetic field pretreatment of adipose-derived stem cells to improve bone healing. J Tissue Eng Regen [Epub ahead of print] DOI: 10.1002/term.1664.
28. Timper, K., Seboek, D., Eberhardt, M., Linscheid, P., Christ-Crain, M., Keller, U., *et al.* Human adipose tissue-derived mesenchymal stem cells differentiate into insulin, somatostatin, and glucagon expressing cells. Biochem Biophys Res Commun **341,** 1135, 2006.
29. Liebner, S., Cattelino, A., Gallini, R., Rudini, N., Iurlaro, M., Piccolo, S., *et al.* β-Catenin is required for endothelial-mesenchymal transformation during heart cushion development in the mouse. J Cell Biol **166,** 359, 2004.
30. Pusztaszeri, M.P., Seelentag, W., and Bosman, F.T. Immunohistochemical expression of endothelial markers CD31, CD34, von Willebrand factor, and Fli-1 in normal human tissues. J Histochem Cytochem **54,** 385, 2006.
31. Gronthos, S., Chen, S., Wang, C.Y., Robey, P.G., and Shi, S. Telomerase accelerates osteogenesis of bone marrow stromal stem cells by upregulation of CBFA1, osterix, and osteocalcin. J Bone Mine Res **18,** 716, 2003.
32. Shu, R., McMullen, R., Baumann, M.J., and McCabe, L.R. Hydroxyapatite accelerates differentiation and suppresses growth of MC3T3-E1 osteoblasts. J Biomed Mater Res A **67A,** 1196, 2003.
33. Peister, A., Deutsch, E.R., Kolambkar, Y., Hutmacher, D.W., and Guldberg, R.E. Amniotic fluid stem cells pro-

duce robust mineral deposits on biodegradable scaffolds. Tissue Eng Part A **15,** 3129, 2009.
34. Meinel, L., Betz, O., Fajardo, R., Hofmann, S., Nazarian, A., Cory, E., *et al.* Silk based biomaterials to heal critical sized femur defects. Bone **39,** 922, 2006.
35. Castano-Izquierdo, H., Alvarez-Barreto, J., van den Dolder, J., Jansen, J.A., Mikos, A.G., and Sikavitsas, V.I. Pre-culture period of mesenchymal stem cells in osteogenic media influences their *in vivo* bone forming potential. J Biomed Mater Res A **82A,** 129, 2007.
36. Khosla, S., Westendorf, J.J., and Modder, U.I. Concise review: insights from normal bone remodeling and stem cell-based therapies for bone repair. Stem Cells **28,** 2124, 2010.
37. Zhang, Z.Y., Teoh, S.H., Chong, M.S.K., Lee, E.S.M., Tan, L.G., Mattar, C.N., *et al.* Neo-vascularization and bone formation mediated by fetal mesenchymal stem cell tissue-engineered bone grafts in critical-size femoral defects. Biomaterials **31,** 608, 2010.
38. Hayashi, N., Peacock, J.W., Beraldi, E., Zoubeidi, A., Gleave, M.E., and Ong, C.J. Hsp27 silencing coordinately inhibits proliferation and promotes Fas-induced apoptosis by regulating the PEA-15 molecular switch. Cell Death Differ **19,** 990, 2012.
39. Havasi, A., Li, Z.J., Wang, Z.Y., Martin, J.L., Botla, V., Ruchalski, K., *et al.* Hsp27 inhibits Bax activation and apoptosis via a phosphatidylinositol 3-kinase-dependent mechanism. J Biol Chem **283,** 12305, 2008.

Address correspondence to:
Dong-Woo Cho, PhD
Department of Mechanical Engineering
Pohang University of Science and Technology (POSTECH)
San 31, Hyoja-dong, Nam-gu
Pohang 790-751
Republic of Korea

E-mail: dwcho@postech.ac.kr

Received: March 5, 2013
Accepted: December 23, 2013
Online Publication Date: February 27, 2014